

In Vivo Evaluation of Cerebral Transplantation of Resovist-Labeled Bone Marrow Stromal Cells in Parkinson's Disease Rats Using Magnetic Resonance Imaging

Jing Guo · Jun-Kang Shen · Lan Wang · Li Xiao ·
Rong-Jun Zhang · Wei-Feng Luo · Zhi-Gang Gong ·
Jing Sun · Han Xu · Pierre Sirois · Kai Li

Received: 27 October 2009 / Accepted: 16 August 2010 /
Published online: 5 September 2010
© Springer Science+Business Media, LLC 2010

Abstract The effectiveness of Resovist-labeled bone marrow stem cells (BMSCs) was evaluated in vivo following their cerebral transplantation in a model of Parkinson's disease (PD) in rats using MRI, and the MRI findings were further compared with the behavior and histopathological manifestations of these rats. Forty PD rats were randomly assigned into five groups according to the cell doses injected into the rat brain site: control group (normal saline injection) and groups injected with 1×10^5 , 1.5×10^5 , 2×10^5 , and 2.5×10^5 BMSCs. Gradient echo T2-weighted images were obtained immediately after cell transplantation and repeatedly taken 1, 4, 8, and 12 week(s) after cell transplantation. The rotational behavior of the animals was observed before and 1, 4, and 8 week(s) after transplantation. The rats were killed after the last MRI scanning, the brain tissues were analyzed by histopathology techniques, and RNAs were extracted for the expression analysis of selected genes using

Jing Guo and Jun-Kang Shen have contributed equally to this paper.

J. Guo · J.-K. Shen (✉) · J. Sun · H. Xu
Department of Radiology, The Second Affiliated Hospital of Soochow University, Suzhou, China
e-mail: junkangsh@yahoo.com.cn

L. Wang · W.-F. Luo
Department of Neurology, The Second Affiliated Hospital of Soochow University, Suzhou 215004,
China

L. Xiao
Department of Laboratory, The Second Affiliated Hospital of Soochow University, Suzhou, China

R.-J. Zhang · Z.-G. Gong
Department of Neurosurgery, The Second Affiliated Hospital of Soochow University, Suzhou, China

P. Sirois
IPS, Sherbrooke University Medical School, Quebec, Canada

K. Li (✉)
The Medical College of Soochow University, Suzhou 215123, China
e-mail: kaili34@yahoo.com

RT-PCR. One week following cell transplantation, all injected sites showed well-defined hypointense areas on MR images, with the most significant effect observed in rats injected with 2×10^5 BMSCs. These MR findings in PD rats lasted up to 12 weeks. The effectiveness of BMSC transplantation revealed by MRI was well confirmed by the behavioral and histopathological observations as well as indirectly supported by gene expression analyses. With the use of SPIO labeling, MRI techniques provided a dynamic evaluation of the spatial and temporal changes following cell transplantation and allowed the association analysis among the imaging, functions, and gene expression analysis in rats. These data also suggest the therapeutic potential of transplanted BMSCs. It is reasonable to speculate that the use of MRI in *in vivo* evaluation of the effect and fate of transplanted cells in various disease models will be beneficial to developing new strategies of cell-based gene therapy.

Keywords BMSCs · Cell transplantation · MRI · PD · Resovist · SPIO

Abbreviations

BMSCs	Bone marrow stem cells
MRI	Magnetic resonance imaging
PD	Parkinson's disease
SPIO	Superparamagnetic iron oxide

Introduction

Parkinson's disease (PD), an age-associated neurodegenerative disease, is characterized pathologically by a dramatic loss of dopaminergic neurons in the substantia nigra of the ventral midbrain and the subsequent deficiency of dopamine in the brain areas [1]. It is manifested as motor impairment with characteristic symptoms including difficulty in initiating movement, rigidity, resting tremor, and postural instability. Little is known about why and how the PD neurodegenerative process begins and progresses. Traditional treatments are largely targeted to symptomatic improvements with drug therapy and surgical interventions. In recent years, cellular transplantation has been suggested to be a promising therapeutic option for patients with PD. Cellular transplantation is an immature strategy under investigation in various animal studies.

Bone marrow stromal cells are multipotent and self-renewing, relatively more accessible than neural stem cells (NSCs) and embryonic stem cells in preparation and *in vitro* proliferation [2]. Similar to NSC in cell therapy for PD [3], a certain subpopulation of BMSCs is known to be capable of differentiating into mesenchymal tissues, including bone, cartilage, fat, tendon, muscle, and marrow stroma *in vitro*. As reported by Woodbury et al. [4], with an optimal differentiation protocol, almost 80% of BMSC could differentiate into neuron-specific enolase (NSE) and neurofilament-M (NF-M) *in vitro*. Additionally, the release of neural growth factors by BMSCs after transplantation into rat brain was observed in a PD model. Based on these findings, it has been suggested that BMSCs could be injected into the striatum and could promote a functional recovery in a mouse model of PD [5].

The development of stem cell-based therapies requires a quantitative and qualitative assessment of stem cell distribution into the target organs, their differentiation outcome, and their migration and engraftment [6]. Currently, most of the techniques used in the study of stem cell transplantation in animal models require histological analysis to determine the fate and migration of the transplanted cells. Once delivered into the striatum, the injected cells

are difficult to visualize and track *in vivo*. Thus, the retention, location, and migration of the transplanted cells can only be estimated postmortem. Radionuclide labels such as ^{111}In has been successfully employed previously in studies of *in vivo* cell trafficking, but the application of these methods in clinical diseases may be limited by the isotopic toxicity to patients [7].

Magnetic resonance (MR) imaging is a noninvasive technology that could provide a high resolution and sensitivity necessary for detecting transplanted cells and allow repetitive investigations without known side effects and without risking radiotoxic damages to the transplanted cells. Since the transplanted cells migrate and differentiate within the host tissues, it is necessary to label the donor BMSCs before transplantation with an MR contrast agent that distinguishes them from host cells for the purpose of experimental evaluation. Superparamagnetic iron oxide (SPIO), a new type of MR contrast agent [8], is adequate to detect small clusters of cells and is not toxic to the cells and the host. BMSCs have been used in labeling experiments and MR tracking *in vivo* [9]. Resovist[®], a FDA-approved MRI contrast agent consisting of SPIO nanoparticles (4–6 nm) [10] coated with carboxydextran (60-nm mean hydrodynamic diameter), could produce predominantly T2 effects, which is seen as a reduction in signal intensity compared with the surrounding white matter, and have produced good MR image contrast [11].

In this study, we labeled the BMSCs with Resovist and transplanted different quantities of the Resovist-labeled BMSC into the brain of PD rats. The distribution of Resovist-positive cells in the brain after transplantation was evaluated to determine the optimal quantity of transplanted BMSCs and the optimal time point for observing with the 1.5-T MR scanner *in vivo*. Significant changes in MR imaging characterized by hypointensive areas were observed for as long as 12 weeks after cell transplantation. The MR findings on these animals were further related to their behavior and to the histopathological observations.

Materials and Methods

BMSCs Isolation and Magnetic Labeling

Sprague–Dawley rats were anesthetized with an intraperitoneal injection of 3.6% chloral hydrate (1 ml per 100 g of body weight). Whole bone marrow was obtained in sterile condition, as described previously [12]. BMSCs were isolated and cultured according to the methods of Colter et al. [13]. Briefly, mononuclear cells were isolated using a density gradient centrifugation, and the culture was expanded based on plastic adherence. The cells were cultured in complete culture solution consisting of 42.5% DMEM medium, 42.5% F12 medium, 15% fetal bovine serum, 100 U penicillin per milliliter, and 100 U streptomycin per milliliter. The non-adherent cells were removed with the change of the medium, and the adherent cells were kept in the culture dish for further growth. The medium was changed every 3 days. When approaching subconfluence (80%), the cells were detached by 0.25% trypsinase treatment to start the cloning procedure with 10% fetal bovine serum medium.

The third generation of BMSCs was incubated with 3 $\mu\text{g}/\text{ml}$ bromodeoxyuridine (BrdU, Sigma, USA) at 37 °C for 72 h. Cell labeling was performed for 48 h with 5.6 $\mu\text{g}/\text{ml}$ SPIO (Resovist, Schering, Germany) in combination with BrdU in standard incubating conditions (37 °C, 5% humidified CO_2). The cells were then detached with 0.25% trypsinase treatment and the collected cells were washed three times with phosphate-buffered saline (PBS) to

remove the unconjugated Brdu and Resovist and suspended with normal saline (NS) to calculate and adjust the cell density (5×10^4 – $10 \times 10^4/\mu\text{l}$) for later use.

To visualize the iron within the BMSCs, Prussian blue staining was performed. Briefly, the cells adhered to the plastic bottom of the culture dish were fixed with 4% paraform, washed, incubated for 30 min with 2% potassium ferrocyanide (Perls agent) in 6% hydrochloric acid, washed, and counterstained with eosin red to visualize the cytoplasm.

Development of the PD Rat Model for Cell Transplantation

Male Sprague–Dawley rats weighing 180–240 g were purchased from Soochow University Experimental Animal Center, China. All experimental procedures were performed according to the “Regulation to the Care and Use of Experimental Animals” (1996) of the Beijing Council on Animal Care.

Altogether, 60 rats were used in the study. They were anesthetized with intraperitoneal injections of 3.6% chloral hydrate (1 ml per 100 g of body weight). The head was fixed on the stereotaxic apparatus (Kopf Instruments, USA) and the dura was exposed at the site of the anterior fontanel. 6-OHDA (8 μl) was injected into the right medial forebrain bundle through two points, as described in the attached Table 1, and then the incision was closed.

Two weeks after the surgery, the rats were selected for PD model estimation by scoring the rotational behavior in response to an injection of apomorphine (0.5 mg/kg, i.p). The number of rotations were counted 10 min after the injection and monitored for 30 min. Rats that presented more than seven rotations per minute ipsilateral toward the side of the damaged brain were considered to be adequate PD rats and were selected for cell transplantation.

Forty out of the 60 operated animals developed an experimental PD. These PD rats were randomly assigned into five groups ($n=8$ each), and each animal received only one injection in the right striatum: control group injected with 20 μl of NS; group 1 injected with 1×10^5 of Resovist-labeled BMSCs; group 2 injected with 1.5×10^5 of Resovist-labeled BMSCs; group 3 injected with 2×10^5 of Resovist-labeled BMSCs; and group 4 injected with 2.5×10^5 of Resovist-labeled BMSCs. Rotational behavior was observed before and 1, 4, and 8 weeks after cell transplantation by counting the numbers of apomorphine-induced head turning of PD rats.

MR Imaging

The initial MR imaging was taken on all rats within 24 h after receiving the cell transplantation of BMSCs labeled with Resovist. Thereafter, MR scans were performed 1, 4, 8, and 12 weeks after the cell transplantation under general anesthesia on a 1.5-T MRI scanner (Philips Achieva System, Holland), with the rat in prone decubitus and Micro-47 coil wrapped around their head. The rats were scanned using a gradient-echo sequence (FFE T2WI) with an echo time of 12 ms and a repetition time of 274 ms. Additional parameters were as follows: section thickness, 1.20 mm; field of view, $60 \times 60 \text{ mm}^2$; base

Table 1 Parameters for the development of the rat model of PD

	Anterior fontanel A-P (mm)	L-R (mm)	Needling depth (mm)	Injection quantity (μl)
Position 1	-1.8(43.1)	-2.5(62.8)	-8(53.5)	4
Position 2	-1.8(43.1)	-2.5(62.8)	-7.5(54)	4

resolution matrix, 256×256 ; and number of signals acquired, 6. Aggregations of labeled cells were reflected as either low-signal-intensity spots or signal voids with gradient-echo sequences.

Histological Analysis

The rats were killed after the MRI analysis 12 weeks after the cell transplantation. Histological analyses were done on brain tissues and a portion was used for localizing the migration of BMSCs following immunohistochemistry staining. Briefly, the PD rats were perfused with normal saline first and then perfused with 4% formaldehyde through the heart; the rat heads were then dissected and fixed under 4% formaldehyde overnight. The brain tissues harboring the abnormal foci revealed by MRI were then sliced at a thickness of 2 mm after gradual dehydration with alcohol. The sliced brain tissues were treated with xylene and then embedded with paraffin.

For BrdU staining, the paraffin-embedded tissues were consecutively sliced at 5 μm for immunostaining analysis. The sliced tissue was first deparaffinized and rehydrated, followed by thermo-inducible retrieval with 0.01 M CB at pH 6.0 by microwave for 20 min and three times PBS washes with intervals of 3 min after it was cooled down to room temperature. Internal peroxidase was inhibited by incubation with 0.3% H_2O_2 for 20 min at room temperature and followed by 3×3 PBS washes. Following block with 20% goat serum for 30 min at room temperature, brain slices were incubated with a 1:100 diluted primary antibody against BrdU for 2 h at 37 $^\circ\text{C}$. Washes with 3×3 PBS were undertaken before and after incubation with EnVision (HRP-M) 37 $^\circ\text{C}$ for 30 min. After visualizing with DAB for 8–12 min, double staining with hematoxylin and washing with PBS were done until slices changed to blue again, then mounted with resins. Photographed under a microscope, cells with nuclei brown stain were positive and those with blue staining were negative.

For Prussian blue staining, the paraffin sections were sliced at 5 μm . After deparaffinization and rehydration, tissue slices were incubated with a mixture solution of 2% potassium ferrocyanide and 6% chloral hydrate for 30 min at room temperature. After being extensively washed with distilled water, the slices were stained with eosine solution 0.5% in water for 30–60 s then gradually dehydrated with alcohol, fixed with xylene, and mounted with plastic cement, and photographed under microscope. Cells with cytoplasmic blue staining (iron particles) were positive.

Gene Expression Analysis with RT-PCR

The corpus striatum was dissected and RNA was extracted for the expression analysis of selected gene by real-time RT-PCR. The levels of mRNA of the neural stem cell marker nestin, the astrocytic marker glial fibrillary acidic protein (GFAP), the neuron marker NSE, or the dopaminergic neuron marker TH was chosen for quantitative analyses. cDNA was submitted to reverse transcription from 5.0 μg total RNA using a random primer and MMLV. Real-time PCR was performed using FTC2000 and SYBR Green I. PCR reactions included 7.5 ng of cDNA, MgCl_2 at the optimal concentration for each gene, 2–2.5 pmol of each primer, 4 μl of SYBR Green I, 1 U of Taq polymerase, and 0.4 μl of dNTP (10 mM) in a final volume of 20 μl . All primers are listed in Table 2. PCR cycling involved melting at 94 $^\circ\text{C}$ for 5 min followed by 35 cycles of 94 $^\circ\text{C}$ for 25 s, 60 $^\circ\text{C}$ for 20 s, and 72 $^\circ\text{C}$ for 30 s, followed by one cycle of 72 $^\circ\text{C}$ for 5 min.

Table 2 Primers sequences

Gene	Primers (5' to 3')	Fragments size (bp)
GFAP	F TGA CTATCGCCG CCAACTGC	127
	R CTGGTAACTCGCCGACTCCC	
Nestin	F GCAGTGCCTGCAAGTAGAAGA	106
	R CTCCCACCGCTGTTGATT	
NSE	F CGTTACTTAGGCAAAGGTGTCC	123
	R CTCCAGCATCAGGTTGTCCAG	
TH	F GGC GACAGAGTCTCATCGAG	139
	R AGAACAGCATTCCCATCCCT	
β -actin	F CCCATCTATGAGGGTTACGC	150
	R TTTAATGTCACGCACGATTC	

The quantity of GFAP mRNA, Nestin mRNA, NSE mRNA, TH mRNA, and β -actin of the samples was calculated according to each standard curve.

Statistical Analysis

Values are expressed as means \pm SEM. Two types of normalization were taken whenever proper. For some longitudinal observation, the value before cell transplantation was used as the baseline for calibration. For gene expression analysis among groups at the time of killing, group with normal saline injection was used as the baseline. Analyses of variance (one-way ANOVA) were performed using SPSS 13.0. A probability value of $P < 0.05$ was considered to denote statistical significance.

Results

The Efficiency of Cells with Resovist Labeling

Prussian blue staining of Resovist-labeled BMSCs revealed the presence of numerous blue staining iron-containing vesicles or particles in the cytoplasm of nearly all cells (Fig. 1). The labeling efficiency reached approximately 97–99% by counting positively stained cells in four independent views with $\times 10$ magnification of more than 1,000 cells.

Dynamic MRI Scanning of Rats with Transplanted Cells

MRI scanning was performed in each of 40 rats: 32 rats were subjected to labeled cell transplantation, whereas eight rats were given a NS injection. When labeled BMSCs were transplanted into the corpus striatum of living rats, FFE T2-weighted MRI images revealed well-defined hypointense areas (dark region) at the site of transplantation (Fig. 2a–d). At the opposite, hypointense areas were not observed on the images from the striatum of the control group in which NS was injected (Fig. 2e). Interestingly, the use of dynamic MRI revealed the extension of the dark region at the fourth week time point in group 3 as compared with the first week time point after cell transplant (Figs. 2c and 3).

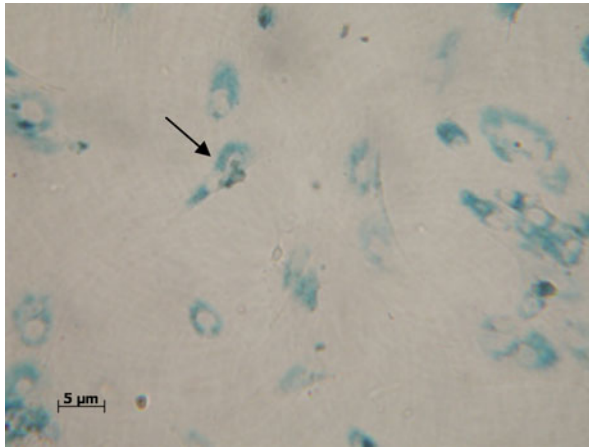


Fig. 1 Prussian blue staining of BMSCs incubated with Resovist ($\times 400$). Following a 48-h incubation with Resovist, the cells stained with Prussian blue showed the presence of numerous blue-stained vesicles or particles in the cytoplasm. The labeled efficiency was approximately 97–99%

In general, however, the hypointense areas were gradually decreased (Figs. 2a–d and 3), but were still observable until the end point of 12 weeks after the cell transplantation in this study. By the end of the study period, 12 weeks after cell transplantation, the images from three rats in group 3 and from one rat in group 4 were still revealing hypointense changes localized in the left ependyma area (Fig. 4a). Although the size of the hypointense areas were positively associated with the number of cells transplanted at the relatively low dose, the most significant hypointense change was observed in the second highest dose of cell transplantation group rather than in the group with highest number of cell transplantation.

Histological Analysis

The cells labeled with Resovist and Brdu could be detected in sections corresponding to hypoenhancing lesions in PD rats scanned with MRI. Prussian blue staining revealed a number of transplanted cells loaded with iron in the right striatum at the time point of 12 weeks after cell transplantation. In the same region, Brdu immunohistochemistry techniques allowed the detection of a large number of Brdu-positive staining cells which were in high density and distributed along the injection site. The transplanted cells migrated extensively from the injected site to the injured regions (Fig. 5). Interestingly, there are a few Brdu-positive cells found in the left ependyma (Fig. 5b) and striatum with which the hypointensive changes on MRI scans were associated.

Gene Expression Analysis with RT-PCR

The real-time quantitative reverse transcription PCR revealed that the quantity of GFAP mRNA was the most abundant (Fig. 6). The quantity of GFAP, NSE, Nestin, and TH mRNA expressed in the third group is more marked compared to that of the other groups, and there is a significant difference between group 3 and the control group ($P < 0.05$, one-way ANOVA). The gene expression levels of these selected genes were significantly increased following cell transplantation, with the most significant increase in the group

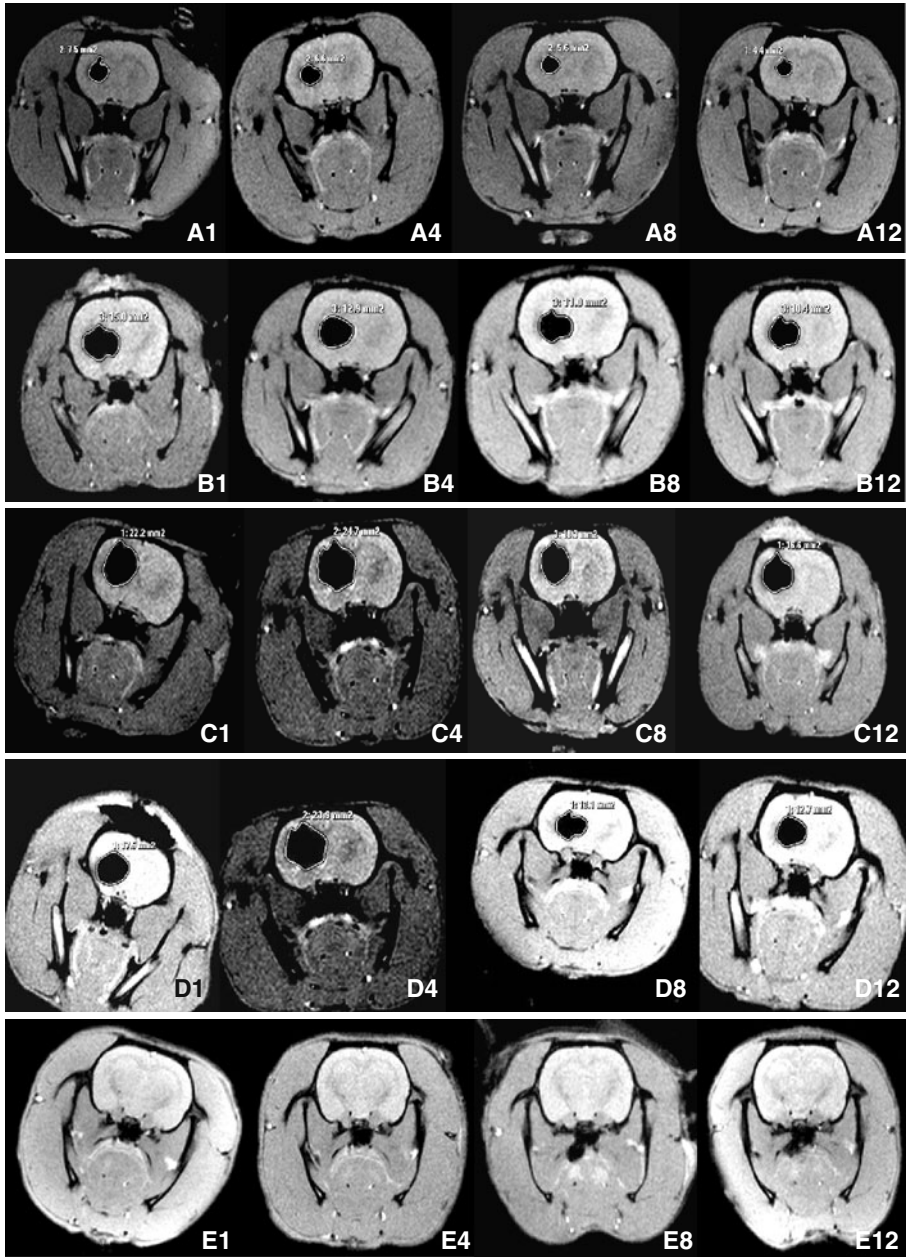


Fig. 2 In vivo signal void in MRI from the brains of PD rats injected with selected amounts of Resovist-labeled BMSCs. MRI scans were performed at 1.5 T. FFE-T2WI sequence. **a–d** Groups of rats injected with 1×10^5 (**a**), 1.5×10^5 (**b**), 2×10^5 (**c**), and 2.5×10^5 (**d**) BMSCs. **e** Control group with saline injection. The subscript digits 1 to 12 showed the number of weeks at which the MRI scans were taken after the cell transplantation. A kind of dose-dependent pattern is illustrated from **a–d** as a function of transplanted cell amount. However, MRI identified the most significant signal void in the group of rats given 2×10^5 BMSCs (**c**)

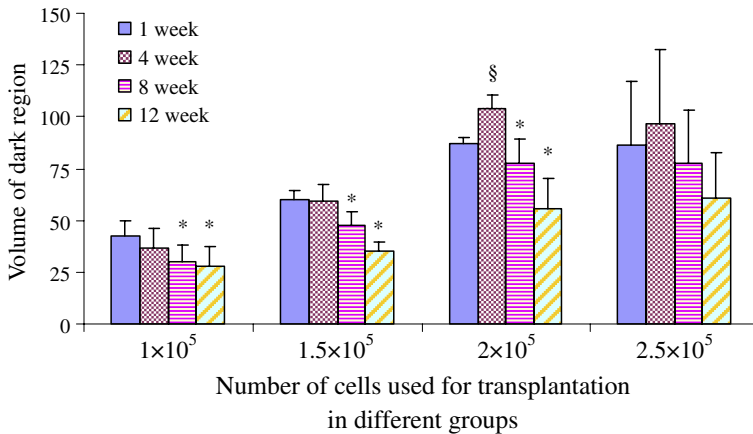


Fig. 3 Volume of dark regions of each group at the selected time point after transplantation. The areas of hypointensity gradually diminished in groups 1 and 2 and became smaller after 4 weeks in groups 3 and 4. *Significant differences between volume of dark region at 1 week and volume of dark region at selected time after transplantation ($P < 0.05$). §The area of hypointense became significant larger at 4 weeks as compared with that at 1 week after transplantation ($P < 0.05$)

following 2×10^5 transplantation. An unexpected low level of gene expression was revealed in the group with the transplantation of the highest number of 2.5×10^5 BMSCs.

Discussion

Stem cell therapies have been intensively studied and have shown to be of potential benefit in the treatment or assessment of many diseases, including hematopoietic diseases, cardiovascular and neurologic diseases, and especially some degeneration disorders, such as PD. In the present study, we performed an in vivo dynamic evaluation of the migratory ability of Resovist-labeled bone marrow stromal cells in a specific brain site in a model of

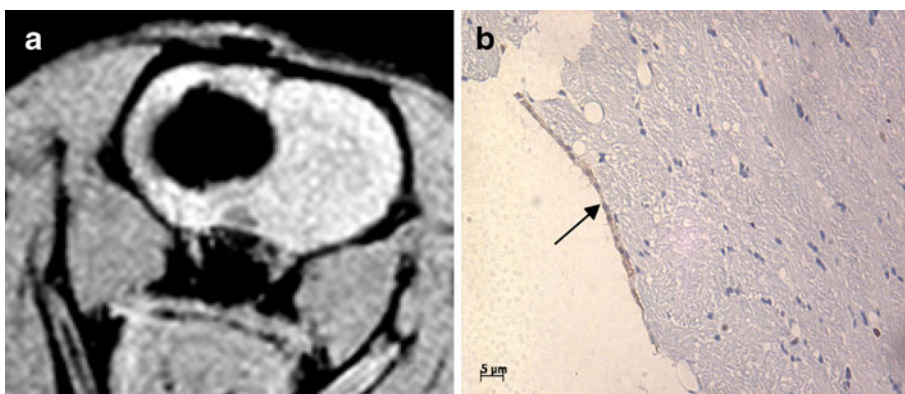


Fig. 4 Hypo-enhancing lesions could be visualized in the left ependyma area at 12 weeks after transplantation of Resovist-labeled BMSCs with MRI scanning (a). b Immunohistochemistry staining revealed that a few cells crossed the midline and migrated toward the left ependyma ($\times 200$ magnification)

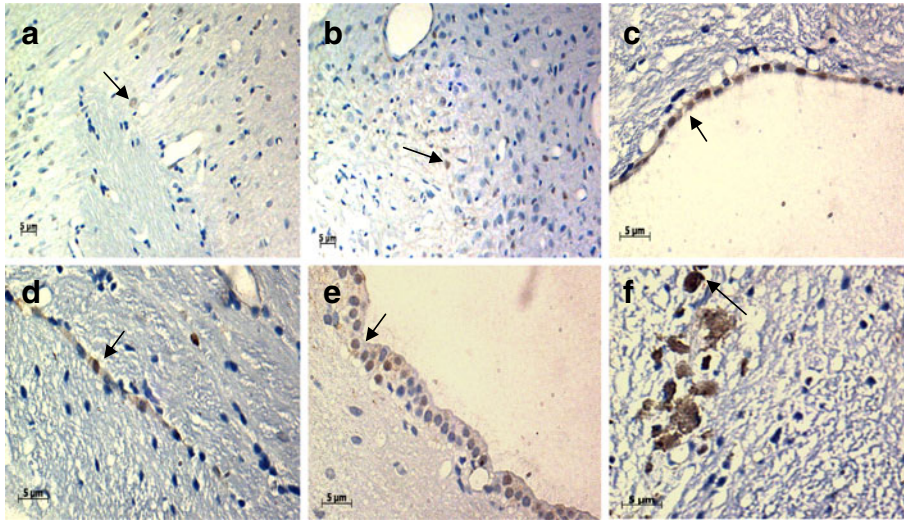


Fig. 5 BrdU immunohistochemistry staining revealed the extensive migration of transplanted cells along specific routes (a–f). There were a number of BrdU positively stained cells in the right striatum (a) (×200 magnification) migrating toward the homolateral cortex (b) (×200 magnifications) and lateral ventricle(c) (×400 magnifications). A few positively stained cells migrated across the corpus callosum (d) (×400 magnification) toward the left endypma (e) (×400 magnification) and striatum (f) (×400 magnification)

PD in rats using MR imaging. The optimal quantity of transplanted cells and observation periods was also determined. The present study demonstrated that BMSCs were amenable for labeling with Resovist, a clinically approved MR contrast agent, and the labeled cells were dynamically detected in the striatum of rats using a standard MR protocol gradient

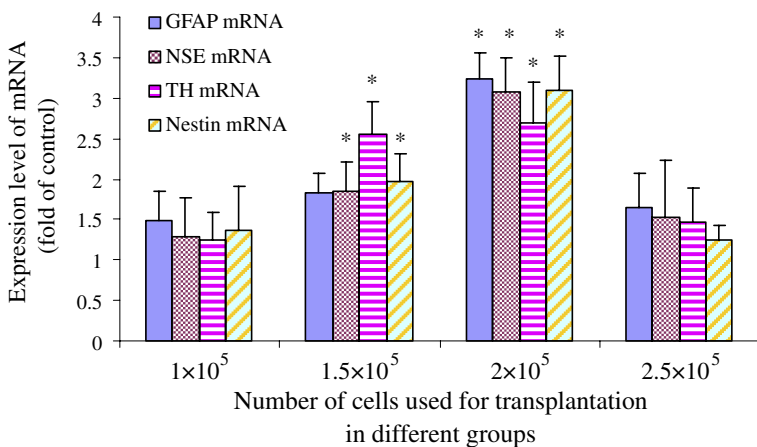


Fig. 6 Quantity of GFAP, NSE, Nestin, and TH mRNA of the selected groups expressed 12 weeks after cell transplantation. *Significant differences between the levels of different mRNA expressions in the experimental groups (groups 1–4) and that in the control group ($P < 0.05$). The values of relative levels of mRNA expressions in experimental groups were calibrated using the average amount of the control group, being 1

echo imaging method (FFE-T2WI). This procedure provided the opportunity of an in vivo study and a longitudinal evaluation of the localization of BMSCs in quite a long time period after their transplantation in the host organism. The present study analyzed the migration route by immunohistochemical staining and dynamically observed the imaging changes following cell transplantation. It seems that the post-transplantation events of BMSCs such as their recruitment, homing, and proliferation—all key mechanisms for achieving successful regenerative cell transplantation—warrant further investigation.

The tracking of BMSCs after their transplantation with the MR imaging technique offers several advantages over conventional methods, including its excellent spatial resolution, high tissue contrast, and the lack of ionizing radiation. Furthermore, although labeling techniques with radiotracers in nuclear medicine (single-photon emission computed tomography, positron emission tomography) could be clinically available and would provide a much higher sensitivity for cell detection than that achieved with MR method, their spatial resolution are limited and temporal resolution for serial follow-up studies would also be limited by the radioactive decay of the tracer. Radiotoxic cell damage could also occur [14]. Furthermore, MR imaging-based cell tracking can be detected for a relatively long time period, even months after the initial labeling procedure.

Superparamagnetic iron oxide particles are ideal agents and possess many of the aforementioned characteristic features. For diagnostic MRI, two acronyms are used for iron-based magnetic particles: SPIO particles and ultra-small SPIO (USPIO) particles; both consist of a crystalline iron oxide core coated with polymers such as dextran, polyethylene glycol, and starch. The intracellular uptake of SPIO is believed to be better than that of USPIO [15–17]. Furthermore, the signal dephasing effects are more pronounced for SPIO-labeled cells than for USPIO-labeled cells, yielding a more intense dephasing of magnetic moments in gradient-echo MR imaging [15]. At present, two compounds within the SPIO family have been approved for clinical use: one of them is under the name of Resovist (or SH-U555A) in Europe and Japan. Resovist is also a very effective and convenient agent for cell labeling without transfection agent [18–20]. Resovist can generate predominantly T2 effects as shown by a reduction in signal intensity compared with the signal of the neighboring normal brain tissue, which enables assessing both immediate and long-term localization with the use of MRI. Gradient-echo sequence such as FFE-T2WI is the most sensitive sequence to tracking SPIO-labeled cells with MRI in vitro and vivo [21–24].

With SPIO labeling, MRI is not only able to detect the success of BMSCs transplantation but is also able to provide a dynamic evaluation of both the spatial and the temporal changes as a result of the cell transplantation. Among the four groups injected with different amounts of cells, the results showed that injection of 2.0×10^5 cells was the most efficient procedure in our experimental conditions. The MRI findings were supported by data from both behavior observations and gene expression analyses. While there were virtually no changes during the 12-week observation period in the normal saline control group, the apomorphine-induced heard turning was significantly decreased during this period in the rats injected with 2.0×10^5 cells (6.81 ± 1.89 in this group vs 0.16 ± 0.13 in normal saline control group, $P < 0.01$). Interestingly, the gene expression data showed a similar pattern, with an increased expression of selected mRNAs in the rats injected with 2.0×10^5 cells (Fig. 6).

There is a dose-dependent pattern with plateau between 2.0×10^5 and 2.5×10^5 BMSCs observed in the present study, which strongly supports the usefulness of in vivo dynamic observation of cell transplantation by MRI in selected animal models. However, one cannot simply consider using 2.0×10^5 cells as an optimal dose of cells for cell-based gene therapy

in rats in different experimental conditions, such as different cell types or disease models. Theoretically, an excellent dose–response pattern should have a plateau effect observed, namely, the biological effect with the highest dose of 2.5×10^5 BMSCs has the same or similar effect of 2.0×10^5 BMSCs. The present study revealed an unexpected decline in the biological effect in the group with transplantation of 2.5×10^5 BMSCs. This could be attributed to the following factors, such as microembolism from aggregated cells, the interference with migration from over viscous cell preparation, toxicities from injured or dead cells injected, or some other factors so far not recognized yet. However, we cannot exclude that the high variability in the group with a high dose of transplanted cells might be an artifact, although it is unlikely possible.

It is known that BMSCs can differentiate into a variety of terminal cells such as astrocytes, neurons, and nerve stem cells. The present study revealed the increased expression of dopaminergic GFAP, NSE, TH, and Nestin following cell transplantation, which would suggest that cell transplantation either upregulates the gene expression of resident cells or some of the transplanted cells might differentiate into the relevant cells. Our histological examination did identify a small amount of the injected cells which migrated in the cortex and even across the midline toward the left ependyma, although the majority of the transplanted cells still remained at or near the injected site in the right striatum.

In conclusion, with the use of SPIO-labeled BMSCs, MRI techniques provided a dynamic evaluation of the spatial and temporal changes in rat brain following cell transplantation. The present study strongly suggests the therapeutic potential of transplanted BMSCs. As somatic cells can be used as stem cells, patient-specific stem cells could be used in cell-based gene therapy in some degenerative diseases. The use of MRI dynamics in the in vivo evaluation of the effect and fate of transplanted cells in various disease models and the possibility of longer observation time will be highly beneficial to developing new strategies of cell-based gene therapy.

Acknowledgments This research was supported by the Natural science fund for colleges and universities in Jiangsu Province (no. 06KJB320097). Mr. Wenbing Li read this manuscript and gave some comments.

References

1. Galvan, A., & Wichmann, T. (2008). Pathophysiology of Parkinsonism. *Clinical Neurophysiology*, *119*, 1459–1474.
2. Sanchez-Ramos, J., Song, S., Cardozo-Pelaez, F., Hazzi, C., Stedeford, T., Willing, A., et al. (2000). Adult bone marrow stromal cells differentiate into neural cells in vitro. *Experimental Neurology*, *164*, 247–256.
3. Daniela, F., Vescovi, A. L., & Bottai, D. (2007). The stem cells as a potential treatment for neurodegeneration. *Methods in Molecular Biology*, *399*, 199–213.
4. Woodbury, D., Schwarz, E. J., Prockop, D. J., & Black, I. B. (2000). Adult rat and human bone marrow stromal cells differentiate into neurons. *Journal of Neuroscience Research*, *61*, 364–370.
5. Li, Y., Chen, J., Wang, L., Zhang, L., Lu, M., & Chopp, M. (2001). Intracerebral transplantation of bone marrow stromal cells in a 1-methyl-4-phenyl-1,2,3,6-tetrahydropyridine mouse model of Parkinson's disease. *Neuroscience Letters*, *316*, 67–70.
6. Strauer, B. E., & Kornowski, R. (2003). Stem cell therapy in perspective. *Circulation*, *107*, 929–934.
7. Read, E. J., Keenan, A. M., Carter, C. S., Yolles, P. S., & Davey, R. J. (1990). In vivo traffic of indium-111-oxine labeled human lymphocytes collected by automated apheresis. *Journal of Nuclear Medicine*, *31*, 999–1006.
8. Corot, C., Robert, P., Idee, J. M., & Port, M. (2006). Recent advances in iron oxide nanocrystal technology for medical imaging. *Advanced Drug Delivery Reviews*, *58*, 1471–1504.

9. Jendelova, P., Herynek, V., Urdzikova, L., Glogarova, K., Kroupova, J., Andersson, B., et al. (2004). Magnetic resonance tracking of transplanted bone marrow and embryonic stem cells labeled by iron oxide nanoparticles in rat brain and spinal cord. *Journal of Neuroscience Research*, *76*, 232–243.
10. Wang, Y. X., Hussain, S. M., & Krestin, G. P. (2001). Superparamagnetic iron oxide contrast agents: Physicochemical characteristics and applications in MR imaging. *European Radiology*, *11*, 2319–2331.
11. Reimer, P., & Tombach, B. (1998). Hepatic MRI with SPIO: Detection and characterization of focal liver lesions. *European Radiology*, *8*, 1198–1204.
12. Javazon, E. H., Colter, D. C., Schwarz, E. J., & Prockop, D. J. (2001). Rat marrow stromal cells are more sensitive to plating density and expand more rapidly from single-cell-derived colonies than human marrow stromal cells. *Stem Cells*, *19*, 219–225.
13. Colter, D. C., Sekiya, I., & Prockop, D. J. (2001). Identification of a subpopulation of rapidly self-renewing and multipotential adult stem cells in colonies of human marrow stromal cells. *Proceedings of the National Academy of Sciences of the United States of America*, *98*, 7841–7845.
14. Fawwaz, R. A., Oluwole, S., Wang, T. S., Kuromoto, N., Iga, C., Hardy, M. A., et al. (1985). Biodistribution of radiolabeled lymphocytes. *Radiology*, *155*, 483–486.
15. Schafer, R., Kehlbach, R., Wiskirchen, J., Bantleon, R., Pintaske, J., Brehm, B. R., et al. (2007). Transferrin receptor upregulation: In vitro labeling of rat mesenchymal stem cells with superparamagnetic iron oxide. *Radiology*, *244*, 514–523.
16. Sun, R., Dittrich, J., Le-Huu, M., Mueller, M. M., Bedke, J., Kartenbeck, J., et al. (2005). Physical and biological characterization of superparamagnetic iron oxide- and ultrasmall superparamagnetic iron oxide-labeled cells: A comparison. *Investigative Radiology*, *40*, 504–513.
17. Metz, S., Bonaterra, G., Rudelius, M., Settles, M., Rummeny, E. J., & Daldrup-Link, H. E. (2004). Capacity of human monocytes to phagocytose approved iron oxide MR contrast agents in vitro. *European Radiology*, *14*, 1851–1858.
18. Linker, R. A., Kroner, A., Horn, T., Gold, R., Maurer, M., & Bendszus, M. (2006). Iron particle-enhanced visualization of inflammatory central nervous system lesions by high resolution: Preliminary data in an animal model. *AJNR. American Journal of Neuroradiology*, *27*, 1225–1229.
19. Henning, T. D., Boddington, S., & Daldrup-Link, H. E. (2008). Labeling hESCs and hMSCs with iron oxide nanoparticles for non-invasive in vivo tracking with MR imaging. *Journal of Visualized Experiments*, *31*, 685. <http://www.ncbi.nlm.nih.gov/pubmed/19066574>.
20. Hsiao, J. K., Tai, M. F., Chu, H. H., Chen, S. T., Li, H., Lai, D. M., et al. (2007). Magnetic nanoparticle labeling of mesenchymal stem cells without transfection agent: Cellular behavior and capability of detection with clinical 1.5 T magnetic resonance at the single cell level. *Magnetic Resonance in Medicine*, *58*, 717–724.
21. Wang, L., Deng, J., Wang, J., Xiang, B., Yang, T., Gruwel, M., et al. (2009). Superparamagnetic iron oxide does not affect the viability and function of adipose-derived stem cells, and superparamagnetic iron oxide-enhanced magnetic resonance imaging identifies viable cells. *Magnetic Resonance Imaging*, *27*, 108–119.
22. Bulte, J. W., Duncan, I. D., & Frank, J. A. (2002). In vivo magnetic resonance tracking of magnetically labeled cells after transplantation. *Journal of Cerebral Blood Flow and Metabolism*, *22*, 899–907.
23. Guzman, R., Uchida, N., Bliss, T. M., He, D., Christopherson, K. K., Stellwagen, D., et al. (2007). Long-term monitoring of transplanted human neural stem cells in developmental and pathological contexts with MRI. *Proceedings of the National Academy of Sciences of the United States of America*, *104*, 10211–10216.
24. George, A. J., Bhakoo, K. K., Haskard, D. O., Larkman, D. J., & Reynolds, P. R. (2006). Imaging molecular and cellular events in transplantation. *Transplantation*, *82*, 1124–1129.